JBUON 2020; 25(6): 2570-2575
ISSN: 1107-0625, online ISSN: 2241-6293 • www.jbuon.com
Email: editorial_office@jbuon.com

ORIGINAL ARTICLE

Correlations of HACE1 expression with pathological stages, CT features and prognosis of hepatocellular carcinoma patients

Zhiqiang Zhang[1], Minmin Teng[2], Zhiying Xu[3], Dewei Wang[4]

[1]Radiology, Zibo Central Hospital, Zibo City, Shandong 255036, China. [2]Image Center, Second People's Hospital of Dezhou City, Dezhou City, Shandong 253000, China. [3]Hematology-Oncology, Linyi County People's Hospital, Dezhou City, Shandong 251500, China. [4]Medical Imaging, People's Hospital of Pingyi County, Linyi City, Shandong 273300, China.

Summary

Purpose: *To explore the correlations of HECT domain and ankyrin repeat-containing E3 ubiquitin protein ligase 1 (HACE1) expression with the pathological stages, computed tomography (CT) features and prognosis of patients with hepatocellular carcinoma (HCC).*

Methods: *The clinical data were randomly collected from 70 patients with primary HCC. The messenger RNA (mRNA) and HACE1 in the cancer and paracancer tissues were determined via real-time quantitative-polymerase chain reaction (qRT-PCR). The curve of the relationship between HACE1 expression and patients' overall survival (OS) was plotted using the Kaplan-Meier method. Finally, the CT imaging data of patients were pooled to analyze the relationships of HACE1 expression with CT signs.*

Results: *Compared with those in the paracancer tissues, the mRNA and protein expression levels of HACE1 declined significantly in HCC tissues ($p<0.05$). It was found through analyzing the clinical indicators that the expression level of HACE1 was considerably correlated with the tumor diameter, tumor-node-metastasis (TNM) stages and pathological grades ($p<0.05$). The survival analysis revealed that the OS of patients in Low HACE1 group was shorter than that in High HACE1 group (median OS: 12.40 months vs. 15.16 months, $p=0.031$). Besides, as indicated by CT examination, the expression of HACE1 was not correlated with the number of tumors ($p>0.05$), but notably associated with the size, capsule and necrosis of tumors ($p<0.05$).*

Conclusions: *HCC tissues are significantly deficient in HACE1, and the combination of HACE1 and CT images may serve as an efficacious strategy for the clinical diagnosis and monitoring of HCC.*

Key words: *HACE1, hepatocellular carcinoma, CT, prognosis*

Introduction

Hepatocellular carcinoma (HCC) is one of the most common malignancies worldwide and ranks second only to lung cancer among all types of tumors for its morbidity rate [1,2]. There were about 782,500 new cases and 745,500 deaths of liver cancer around the world in 2012 [2]. The total cases and deaths of HCC in China where liver cancer is prevalent account for 50% of those worldwide [3]. Surgery and liver transplantation remain the most suitable treatment options for patients. However, at diagnosis HCC has progressed to advanced stage and cannot be surgically resected in most patients [4]. Considering the poor prognosis of liver cancer, novel treatment strategies and targets are needed, but the major pathogenic genes and molecular mechanism of HCC have not yet been elucidated by studies. Additionally, the incidence rate of HCC is increasing with the aging of population and environmental pol-

Corresponding author: Dewei Wang, BM. Medical Imaging, People's Hospital of Pingyi County, No. 7 Jinhua Rd, Pingyi, Linyi City, Shandong 273300, China
Tel: +86 15020920920, Email: qi2521@163.com
Received: 10/10/2020; Accepted: 02/11/2020

lution [5]. Therefore, searching the pathogenic genes and molecular mechanism of HCC is crucial for the prevention and treatment of this disease.

According to a study, HECT domain and ankyrin repeat-containing E3 ubiquitin protein ligase 1 (HACE1) gene, located on human chromosome 6q21, is a frequently mutated locus in malignant tumors [6]. HACE1 was firstly reported to be closely associated with the development of Wilms tumor [7]. Later, some studies have demonstrated that HACE1, an important tumor suppressor gene, mediates cell autophagy, and ubiquitination of RAC1 to play a vital role in suppressing tumors [8,9]. Moreover, HACE1 is implicated in multiple biological processes, such as cardioprotection, anti-oxidative stress and cell dynamics [10]. A recent study uncovered that low expression or mutation of HACE1 is associated with various human malignancies, including breast cancer, colorectal cancer and lymphoma [11]. However, there have been few data on the biological role and clinical significance of HACE1 in HCC.

Therefore, in the present study 70 HCC patients were randomly recruited and the differences in the transcriptome and protein expression levels of HACE1 between the cancer and paracancer tissues were detected using real-time quantitative polymerase chain reaction (qRT-PCR) and immunohistochemistry (IHC), respectively. Besides, the correlations of HACE1 with the clinical indicators of HCC and its role in the prognosis of HCC patients were evaluated. Importantly, this study firstly combined HACE1 expression with the computed tomography (CT) signs of patients to comprehensively explore the role of HACE1 in HCC.

Methods

Clinical data of samples

The clinical data and the paired specimens of tumor tissues and adjacent non-tumor tissues (5 cm away from the tumors) were randomly collected from 70 patients with primary HCC, who had undergone conventional hepatectomy in our hospital from May 2011 to July 2019. Fresh tissues were divided into 2 portions: one was cryopreserved in liquid nitrogen and the other was immediately fixed in 4% paraformaldehyde overnight and embedded in paraffin. Among these patients, there were 46 males and 24 females, aged 30-78 years old, with median age of 61 years old. The histology of tumor tissues was evaluated independently by two pathologists. The clinicopathological data, including age, gender, levels of serum AFP and ALT, tumor size and number, vascular invasion, HBsAg, tumor differentiation and cirrhosis and CT imaging data were collected from all the patients. This study was approved by the Ethics Committee of Zibo Central Hospital. Signed informed consents were obtained from all participants before the study entry.

Determination of HACE1 messenger ribonucleic acid (mRNA) level via qRT-PCR

Following tissue homogenization, total RNAs were isolated from the tissues using TRIzol reagent (TaKaRa, Tokyo, Japan). Then, first-strand complementary deoxyribose nucleic acids (cDNAs) were synthesized using the reverse transcription system kit (GeneCopoeia, Guangzhou, China), and subjected to qRT-PCR using the standard SYBR PCR kit in StepOnePlus system (Applied Biosystems, Foster City, CA, USA). HACE1 sense sequence: 5'-TCTTACAGTTTGTTACGGGCAGTT-3', antisense sequence: 5'-CAATCCACTTCCACCCATGAT-3'. GAPDH sense sequence: 5'-GGGAGCCAAAAGGGTCAT-3', antisense sequence: 5'-GAGTCCTTCCACGATACCAA-3'. This experiment was performed in triplicate and the fold change of gene expression was calculated using $2^{-\Delta\Delta Ct}$.

Measurement of HACE1 protein level via IHC

The paraffin-embedded tissues were sliced into 4 μm-thick sections, baked in an oven at 60°C for 30 min, de-paraffinized in xylene and hydrated. Then, the sections were permeabilized by 5% Triton for 30 min and added with citric acid buffer (pH=6.0), followed by 15 min of microwave antigen retrieval. Subsequently, endogenous peroxidases were blocked using 3% H_2O_2-containing deionized water. The resulting sections were sealed by 5-10% normal goat serum diluted by phosphate buffered saline (PBS) and incubated at room temperature for 10 min, and then with 100 μL of HACE1 primary antibody (1:200, product No.: ab133637, Abcam, Cambridge, MA, USA) at 4°C overnight, with the PBS as the negative control of the primary antibody. On the next day, the slides were rinsed using PBS, added dropwise with horseradish peroxidase-labeled secondary antibody, incubated at room temperature for 30 min and stained by the GTVision anti-mouse/rabbit antibody complex method and GTVison detection system kit (Gene Tech Co., Ltd., Shanghai, China). The presence of yellow particles in cells indicated positive expression. Finally, images of each section were randomly captured in 10 randomly selected different fields of view under a microscope, and the positive cells were counted, followed by calculation of the positive rate.

Semi-quantitative scoring was performed for positive cells whose cytoplasm was stained brown or tan from the following two aspects: (1) Degree of staining: 0 points for no stain, 1 point for slightly staining, 2 points for moderately staining and 3 points for deeply staining. (2) Percentage of stained cells: 0 points for no stained cells, 1 point for <25% stained cells, 2 points for 25-50% stained cells and 3 points for >50% stained cells. The total score was obtained by adding the points from these two aspects (0-6 points). 0-2 points represented negative expression, while over 2 points indicated positive expression.

CT examination

Double spiral CT scanning was performed using the CT-Twin scanner (Elscint, Israel) at the reconstruction matrix of 512×512, the conventional slice thickness of 10 mm, and an increase of 5 mm for thin slice scanning in affected zones, and contrast-enhanced scans were adopted for the affected zones in some patients. In the present

study, the conventional CT findings were statistically analyzed. Spiral CT data were assessed independently by two radiologists by the double-blind method. Finally, the imaging results of all the patients were compared with their histopathological examination results.

Statistics

SPSS 20.0 software (IBM, Armonk, NY, USA) was employed for analyses. The correlations of the positive rate of HACE1 protein with the clinicopathological variables were analyzed using chi-square (x^2) test. Overall survival (OS) curves were plotted using the Kaplan-Meier method and analyzed by log-rank test. The differences were considered to be statistically significant at $p<0.05$.

Results

MRNA and protein expression levels of HACE1 in HCC tissues and paracancer tissues determined by qRT-PCR and IHC

The protein expression of HACE1 was assessed using the IHC score. Compared with that in the paracancer tissues, the protein of HACE1 was negatively expressed in the 49 out of 70 (70%) cases of HCC tissues, while the positive expression rate of HACE1 was only 30% (21/70), with a statistically significant difference ($p<0.05$) (Figure 1A). The mRNA and pro-

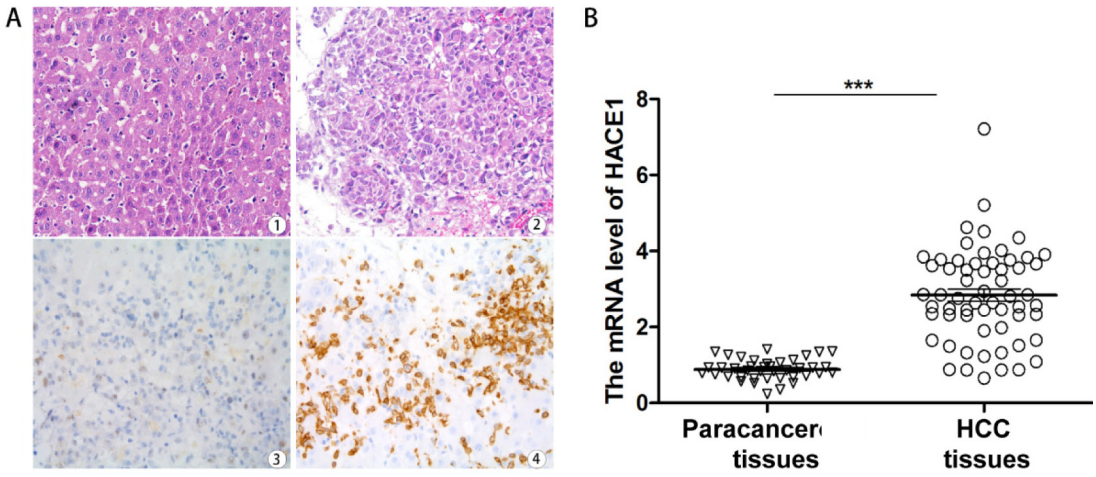

Figure 1. mRNA and protein expression levels of HACE1 in the HCC and paracancer tissues determined via qRT-PCR and IHC, respectively. **A:** HACE1 was mainly expressed in the cytoplasm, and the positive cells were stained brown or tan. (A-1) & (A-3) Paracancer tissues. (A-2) & (A-4) The paired HCC tissues. **B:** HACE1 mRNA expression level in the HCC and paracancer tissues determined via qRT-PCR. The expression of HACE1 obviously declined in the HCC tissues ($p<0.05$), and the mean fold change of HACE1 mRNA expression level in HCC tissues/that in the paracancer tissues was 0.48 (***$p<0.05$).

Table 1. Correlations of HACE1 expression with clinical indicators of HCC patients

Clinical indicators	*n=70*	*High HACE1 group (n=21)*	*Low HACE1 group (n=49)*	x^2	*p*
Age (years)				0.537	0.463
<60	32	11	21		
≥ 60	38	10	28		
Gender				1.461	0.227
Male	46	16	30		
Female	24	5	19		
Tumor diameter (cm)				11.168	0.000832
<5	18	11	7		
≥5	52	10	42		
TNM stage				11.473	0.000706
I-II	23	13	10		
III-IV	47	8	39		
Pathological grade				9.247	0.00185
Low	38	8	30		
Moderate	20	7	13		
High	12	6	6		

tein expression levels of HACE1 in 70 pairs of HCC tissue and adjacent non-tumor tissue specimens were evaluated using qRT-PCR and IHC, respectively. The expression of HACE1 obviously declined in the HCC tissues ($p<0.05$). The mean fold change of HACE1 mRNA expression level in HCC tissues/that in the paracancer tissues was 0.48 (Figure 1B).

Correlations of HACE1 expression with clinical indicators of HCC patients

The expression of HACE1 in the tumor tissues of 70 HCC patients was not associated with their age and gender ($p>0.05$), but it was remarkably correlated with the tumor diameter, TNM stages and pathological grades ($p<0.05$) (Table 1).

CT signs of HCC patients

In the plain CT scanning images, low-density foci with clear boundary and irregular morphology as well as pseudocapsule were found, and calcification was seen inside some foci. There were few cases of a single large lump in the liver, with small satellite foci, double foci and diffuse multiple foci around. Besides, the contrast-enhanced CT scans showed that tumor parenchyma were persistently enhanced in the arterial and venous phases, while the central scar tissues were not enhanced, with low density (Figure 2).

Relationships of HACE1 expression with CT signs of HCC patients

Table 2 presents the relationships of the tumor size, number, capsule and necrosis as shown in CT scans with HACE1 protein expression. Based on the CT findings, there were 54 cases of ≥5 cm tumors, 14 cases of a single lump and 56 cases of multiple lumps (2-5 nodes). The tumors had intact capsules in 21 cases, and incomplete capsules were detected in 49 cases. Additionally, tumor necrosis was found in 40 cases.

Figure 2. CT signs of HCC patients. Figure 2 show the CT imaging data of an HCC patient diagnosed with a space-occupying lesion in the left lobe of the liver. Besides, a quasi-circular uneven isodensity focus with a less defined boundary and low-density capsules were found in the left lobe of the liver. **A:** Fast-in and fast-out enhancement pattern was adopted, which showed that the focus was obviously evenly enhanced with a density higher than that of liver parenchyma in the arterial phase. **B:** The density was slightly decreased in the portal venous phase. **C:** The focus had a slightly lower density in the delayed phase and a far lower density area inside, with an enhanced and higher-density capsule.

Table 2. Correlations of HACE1 expression with CT signs of HCC patients

CT signs	*n (70)*	*Expression of HACE1*		x^2	*p*
		High expression	*Low expression*		
Tumor size, cm				20.000	<0.0001
<5	16	12	4		
≥5	54	9	45		
Tumor number				3.333	0.0678
Single	14	7	7		
Tumor capsule				37.080	<0.0001
Multiple	56	14	42		
Intact	21	17	4		
Incomplete	49	4	45		
Tumor necrosis zone				22.500	<0.0001
Yes	40	3	37		
No	30	18	12		

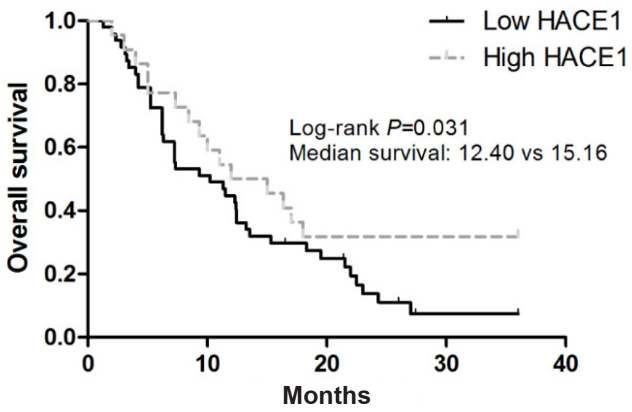

Figure 3. Relationship between HACE1 protein expression and prognosis of HCC patients. The OS of patients in Low HACE1 group was shorter than that in High HACE1 group (p<0.05), and the median OS was 12.40 months in Low HACE1 group and 15.16 months in High HACE1 group (p=0.031 in the log-rank test).

The expression of HACE1 was not correlated with the number of tumors as indicated by CT examination (p>0.05), but was notably associated with the size, capsule and necrosis of tumors (p<0.05).

Correlation between HACE1 protein expression and prognosis of HCC patients

The curve of the relationship between the expression of HACE1 and the OS of patients was plotted using the Kaplan-Meier method. According to the results (Figure 3), the patients in Low HACE1 group had a shorter OS than those in High HACE1 group (p<0.05), indicating that the loss of HACE1 expression is associated with the poor prognosis of patients. The median OS was 12.40 months in Low HACE1 group and 15.16 months in High HACE1 group (p=0.031 in the log-rank test).

Discussion

Human chromosome 6q21 contains one or more major tumor suppressor genes. HACE1 gene encodes a 103 kDA protein that contains 6 N-terminal repeats linked to the C-terminal HECT domain [12]. The expression of HACE1 gene, located on chromosome 6q21, is down-regulated or lost in multiple human tumors, such as Wilms tumor, breast cancer and lung cancer. According to the results of previous studies, the low expression or loss of HACE1 is caused by its ubiquitination or methylation and associated with the development and invasion of different types of cancers. It can be inferred from these results that HACE1 is a novel candidate tumor suppressor gene and may serve as a treatment target for several kinds of human cancers [13,14]. However, the expression of HACE1 and its biological role and clinical significance in HCC remain to be further studied.

In this study, the clinical and pathological specimens were collected from 70 cases of primary HCC. First, it was found that the mRNA transcription and protein expression levels of HACE1 were considerably down-regulated in HCC tissues. The study of Goka et al [15] suggested that the expression of HACE1 in breast cancer tissues is correlated with tumor differentiation and vascular invasion. Likewise, the loss of HACE1 in the tumor tissues was closely related with larger tumor diameter, higher TNM stages and higher pathological grades in 70 HCC patients in the present study. Besides, consistent with the gastric cancer study results of Qu et al [16], the survival analysis results showed that the patients in Low HACE1 group had a lower OS rate than those in High HACE1 group. Therefore, it is believed that HACE1 plays an important role in the development and progression of HCC.

However, detection of biomarkers combined with imaging examination has long been one of the important methods for the clinical diagnosis and treatment of HCC [17]. In particular, focal hepatic lesions need to be screened out regularly for the patients with chronic liver diseases, such as hepatitis B and cirrhosis, which are likely to progress into HCC. CT is important for the diagnosis of HCC [18]. Plain CT scanning images are mainly characterized by low-density foci with clear boundaries and irregular morphology as well as pseudocapsules, and calcification in some foci. Most HCC patients have round or oval low-density foci and infiltrating tumors with undefined boundaries and no capsules. Besides, there are few cases of a single large lump in the liver, with small satellite foci, double foci and diffuse multiple foci around, and ischemic necrosis, bleeding and calcification can be observed in the central tumor cells of foci [19]. Contrast-enhanced CT scanning images sometimes show enhancement of enlarged lymph nodes in the hepatic hilum and abdominal cavity and persistent enhancement of tumor parenchyma in the arterial and venous phases, as well as low-density tumor thrombi. Moreover, filling defect is observed in the tumor thrombi of the hepatic vein and inferior vena cava, in which importantly, lymph node metastasis is also found. However, foci cannot be distinguished by CT scanning well in the early-stage liver cancer patients with tumor diameter <1 cm [20]. In addition, the differences in blood supply to liver cancer, pathological types and

cell differentiation makes it necessary to combine pathological examination with detection of serum biomarkers for diagnosis. In the present study, the CT findings manifested that there were 54 cases of ≥5 cm tumors, 14 cases of a single lump and 56 cases of multiple lumps (2-5 nodes). Besides, intact capsules and incomplete capsules were found in 21 cases and 49 cases, respectively, and tumor necrosis was observed in 40 cases. The expression of HACE1 was not correlated with the number of tumors as indicated by CT examination ($p>0.05$), but was notably associated with the size, capsule and necrosis of tumors ($p<0.05$), which has not yet been reported at present.

Conclusions

In conclusion, the preliminary data of this study reveal that HACE1, a tumor suppressor gene, is significantly lost in HCC tissues and indicates poor prognosis of patients. Importantly, HACE1 expression is closely associated with CT imaging features and its combination with CT imaging may be a potent strategy for the clinical diagnosis and monitoring of HCC.

Conflict of interests

The authors declare no conflict of interests.

References

1. Sagawa T, Kogiso T, Sugiyama H, Hashimoto E, Yamamoto M, Tokushige K. Characteristics of hepatocellular carcinoma arising from Fontan-associated liver disease. Hepatol Res 2020;50:853-62.
2. Zhang S, Liu Y, Liu Z et al. CircRNA_0000502 promotes hepatocellular carcinoma metastasis and inhibits apoptosis through targeting microRNA-124. JBUON 2019;24:2402-10.
3. Ho SY, Liu PH, Hsu CY et al. Evolution of etiology, presentation, management and prognostic tool in hepatocellular carcinoma. Sci Rep 2020;10:3925.
4. Liu Z, Zhang Y, Xu Z. UNC119 promotes the growth and migration of hepatocellular carcinoma via Wnt/beta/catenin and TGF/beta-EMT signaling pathways. JBUON 2018;23:188-92.
5. Kapiris I, Nastos K, Karakatsanis A et al. Survivin expression in hepatocellular carcinoma. Correlation with clinicopathological characteristics and overall survival. JBUON 2019;24:1934-42.
6. El-Naggar AM, Clarkson PW, Negri GL et al. HACE1 is a potential tumor suppressor in osteosarcoma. Cell Death Dis 2019;10:21.
7. Jia W, Deng Z, Zhu J et al. Association Between HACE1 Gene Polymorphisms and Wilms' Tumor Risk in a Chinese Population. Cancer Invest 2017;35:633-8.
8. Kim I, Shin SH, Lee JE, Park JW. Oxygen sensor FIH inhibits HACE1-dependent ubiquitination of Rac1 to enhance metastatic potential in breast cancer cells. Oncogene 2019;38:3651-66.
9. Deng HX. HACE1, RAC1, and what else in the pathogenesis of SPPRS? Neurol Genet 2019;5:e326.
10. Razaghi B, Steele SL, Prykhozhij SV et al. hace1 Influences zebrafish cardiac development via ROS-dependent mechanisms. Dev Dyn 2018;247:289-303.
11. Zhou Z, Zhang HS, Zhang ZG et al. Loss of HACE1 promotes colorectal cancer cell migration via upregulation of YAP1. J Cell Physiol 2019;234:9663-72.
12. Chen YL, Li DP, Jiang HY et al. Overexpression of HACE1 in gastric cancer inhibits tumor aggressiveness by impeding cell proliferation and migration. Cancer Med 2018;7:2472-84.
13. Zhang Z, Zhang R, Zhu J et al. Common variations within HACE1 gene and neuroblastoma susceptibility in a Southern Chinese population. Onco Targets Ther 2017;10:703-9.
14. Tortola L, Nitsch R, Bertrand M et al. The Tumor Suppressor Hace1 Is a Critical Regulator of TNFR1-Mediated Cell Fate. Cell Rep 2016;16:3414.
15. Goka ET, Lippman ME. Loss of the E3 ubiquitin ligase HACE1 results in enhanced Rac1 signaling contributing to breast cancer progression. Oncogene 2015;34:5395-5405.
16. Qu Y, Dang S, Hou P. Gene methylation in gastric cancer. Clin Chim Acta 2013;424:53-65.
17. Tegel BR, Huber S, Savic LJ et al. Quantification of contrast-uptake as imaging biomarker for disease progression of renal cell carcinoma after tumor ablation. Acta Radiol 2020:19835532.
18. Gupta A, Kumar R, Yadav HP et al. Feasibility of 4D CT simulation with synchronized intravenous contrast injection in hepatocellular carcinoma. Rep Pract Oncol Radiother 2020;25:293-8.
19. Nie P, Yang G, Guo J et al. A CT-based radiomics nomogram for differentiation of focal nodular hyperplasia from hepatocellular carcinoma in the non-cirrhotic liver. Cancer Imaging 2020;20:20.
20. El-Hachem N, Habel N, Naiken T et al. Uncovering and deciphering the pro-invasive role of HACE1 in melanoma cells. Cell Death Differ 2018;25:2010-22.